The Effect of Temperature on the Structure of Gaseous Molecules. 3. Molecular Structure and Barrier to Internal Rotation for Diboron Tetrafluoride

Donald D. Danielson, James V. Patton, and Kenneth Hedberg*

Contribution from the Department of Chemistry, Oregon State University, Corvallis, Oregon 97331. *Received October 14, 1976*

The molecular structure of gaseous B_2F_4 has been investigated by electron diffraction at nozzle-tip temperatures of −50, 22, and 150 °C. In contrast to B_2Cl_4 which is staggered in the gas phase, the B_2F_4 molecule has a planar equilibrium conformation (symmetry D_{2h}). The effect of temperature change on the amplitude of the torsional motion is remarkable and commensurate with a description of this motion as slightly hindered internal rotation. The principal bond lengths (r_a), bond angles, and rms amplitudes (l) at 22 °C with uncertainties estimated at 2σ are r(B–B) = 1.720(4) Å, r(B–F) = 1.317(2) Å, ∠BFF = 121.4(1)°, l(B–B) = 0.0499(87) Å, l(B–F) = 0.0459(23) Å, l(B · · · F) = 0.0735(40) Å, and l(F · · · F in BF_2) = 0.0561(31) Å. The average value for the rotational barrier V_0 from the three temperatures is 0.42(16) kcal/mol based on an assumed hindering potential of the form $2V = V_0(1 - \cos 2\phi)$. The estimated value of the fundamental torsional frequency is 19(4) cm^{-1}. The different conformations of B_2F_4 and B_2Cl_4 are discussed in terms of a different balancing of the effects of conjugation tending to favor the planar form and steric interactions favoring the staggered.

It is well known that the diboron tetrahalide molecules consist of two BX_2 groups joined by a B–B bond. Detailed structure determinations of crystalline B_2F_4[1] and B_2Cl_4[2] and gaseous B_2Cl_4[3] have shown that the arrangement of the four atoms comprising the BBX_2 sets is a coplanar one, and that the B–X bond lengths and the XBX bond angles differ only slightly from those in the corresponding boron trihalides. In addition to these structural similarities, however, there is a curious structural difference: In crystalline B_2F_4 and B_2Cl_4 the BX_2 groups are eclipsed (molecular symmetry D_{2h}) whereas in gaseous B_2Cl_4 they are staggered (symmetry D_{2d}).

The eclipsed conformation of crystalline B_2Cl_4 seems clearly to be the result of packing forces on an otherwise staggered molecule with a low barrier (1.8 kcal/mol)[3,4] to internal rotation. Since the staggered and eclipsed conformations themselves imply rather different intramolecular properties, the gas-phase structure of B_2F_4 becomes an important question. Spectroscopic data have been gathered for B_2F_4 in both gas[5-7] and solid[5,7] phases as well as in matrix isolation.[8] Interpretations of data from the earlier studies[5,6,8] as well as results of theoretical calculations[9-11] are in disagreement about the molecular conformation; however, the later infrared and Raman work[7] revealed no violation of the mutual exclusion rule suggesting D_{2h} symmetry for the molecule in both gas and solid phases.

Some years ago, two of us undertook a gaseous electron-diffraction study of B_2F_4. Although that work was never completed, most of the structural details had become clear including the molecular conformation (D_{2h})[12] and the fact that the rotational barrier was much lower than in B_2Cl_4. Recently, we decided to reanalyze our data. More powerful procedures developed in the interim promised a more accurate estimate of the parameter values and of the rotational barrier height. Our results are described herein.

Experimental Section

Diffraction Experiments. Samples of B_2F_4 were prepared and purified by procedures described previously.[5] About 30 diffraction photographs were made in the Oregon State apparatus with an r^3 sector at three nominally different[13] nozzle-tip temperatures using 8 × 10 in. and 5 × 7 in. Kodak projector slide (medium contrast) plates developed for 10 min in D-19 developer diluted 1:1. Exposures were made for 0.5–4.0 min with pressures in the apparatus from 2.1×10^{-6} to 5.0×10^{-6} Torr at nozzle-to-plate distances of 74.836–74.880 cm (long camera) and 30.004–30.020 cm (middle camera). Undiffracted beam currents were 0.06–0.30 μA with wavelengths from 0.05689 to 0.05768 Å (as calibrated from CO_2 diffraction patterns: r_a(CO) = 1.1646 Å, r_a(OO) = 2.3244 Å). In the beginning many of the developed plates were found to have been ruined by yellow stains, a phenomenon which has occurred in this laboratory on only two other occasions—both, incidentally, also involving boron compounds.[14] The problem was largely overcome by rinsing the plates in water just before development. Twelve plates were selected for the structure analysis.

Reduction of Data and Radial Distribution Curves. The procedures for obtaining the scattered intensity distribution s^4I_T have been described.[15] Those procedures were followed except for the case of one plate, made at the intermediate distance in the 22 °C experiment, which could not be rotated during microdensitometry because of a blemish. For it seven diametrical scans in different directions were averaged to provide data comparable to those from the other plates. Experimental backgrounds were calculated[16] and subtracted to provide molecular intensity data in the form represented by

$$sI_m(s) = k \sum_{i \neq j} A_i A_j r_{ij}^{-1} \cos |\eta_i - \eta_j| V_{ij} \sin s(r_{ij} - \kappa_{ij} s^2) \quad (1)$$

The range of the data was $1.00 \leq s < 32.5$. Curves of the total scattered intensities, the final backgrounds, and the molecular intensities are shown in Figures 1–3; the data for these curves are available as supplementary material (see paragraph at end of text regarding supplementary material).

Radial distribution curves were calculated from composite intensity curves according to

$$rD(r) = \frac{2}{\pi} \Delta s \sum_{s=0}^{s_{max}} I'(s) \exp(-Bs^2) \sin rs \quad (2)$$

with $I'(s) = sI_m(s) Z_B Z_F A_B^{-1} A_F^{-1}$ and $B = 0.0025$ Å^2. The modified scattering amplitudes A_i were obtained[15] from tables.[17] For the experimental radial distribution curves data for the unobserved or uncertain region $s < 1.00$ were taken from theoretical intensity curves. The final radial distribution curves are shown in Figure 4.

Structure Analysis

The equilibrium coplanar structure of gaseous B_2F_4 known from the older work is clearly evident from the radial distribution curves: The two peaks at 3.1 and 3.8 Å corresponding to the cis and trans F · · · F distances would have been a single peak at about 3.4 Å in a staggered conformation.

Refinements of the structures were carried out by least squares based on intensity curves[18] in the form of eq 1 adopting the harmonic-vibration approximation $V_{ij} = \exp(-l_{ij}^2 s^2/2)$ and $\kappa = 0$. A single theoretical intensity curve was adjusted simultaneously, using a unit weight matrix, to all individual sets of data obtained at one temperature. The geometrical

Table I. Structural Results for B_2F_4[a]

	−50 °C		22 °C		150 °C	
	r_a	l	r_a	l	r_a	l
B–F	1.314 (2)	0.0393 (20)	1.317 (2)	0.0459 (23)	1.314 (1)	0.0425 (21)
B–B	1.719 (4)	0.0569 (89)	1.720 (4)	0.0499 (87)	1.718 (4)	0.0541 (76)
B ··· F	2.652 (4)	0.0659 (36)	2.656 (4)	0.0735 (40)	2.651 (4)	0.0822 (44)
$F_1 \cdots F_2$	2.245 (3)	0.0494 (28)	2.247 (3)	0.0561 (31)	2.245 (3)	0.0569 (30)
$F_1 \cdots F_3$	3.817 (10)	0.0628[b] } (93)	3.823 (10)	0.0652[b] } (109)	3.816 (11)	0.0808[b] } (142)
$F_2 \cdots F_3$	3.087 (10)	0.1266 }	3.093 (10)	0.1403 }	3.086 (11)	0.1725 }
∠BFF	121.4 (1)		121.4 (1)		121.4 (1)	
∠FBF	117.3 (2)		117.2 (2)		117.3 (2)	
V_0	0.482 (130)		0.353 (161)		0.322 (279)	
R[c]	0.072		0.059		0.065	

[a] Distances (r) and amplitudes (l) in angströms, angles in degrees, V_0 in kcal/mol. Parenthesized values are 2σ. [b] Refined as a group with constant difference. [c] $R = [\Sigma w_i \Delta_i^2 / \Sigma w_i (I_i^{obsd}(s))^2]^{1/2}$ where $\Delta_i = I^{obsd}(s) - I_i^{calcd}(s)$.

Table II. Correlation Matrix for Final Model at 22 °C (× 10^3)[a]

	r_{B-B}	r_{B-F}	∠FBF	l_{B-B}	l_{B-F}	$l_{B \cdots F}$	$l_{F(1)F(2)base}$	$l_{F(2)F(3)}$	V_0
σ_{LS}[b]	1.20	0.29	69.4	3.00	0.49	0.93	0.76	3.56	5.70
	1000	−482	500	32	−63	−79	−10	−72	−30
		1000	−562	−67	−3	47	−37	−49	−60
			1000	10	46	−27	19	−4	0
				1000	95	47	215	40	17
					1000	309	368	89	−5
						1000	125	4	−35
							1000	85	19
								1000	682
									1000

[a] Distances and amplitudes in angstroms, angle in degrees, barrier in kcal/mol. [b] From least-squares refinement.

parameters were taken as the two bond distances and the BBF bond angle. The amplitude parameters, l_{ij}, were those associated with the four torsion-insensitive distances and a fifth, discussed below, of somewhat more complicated character associated with the torsion-sensitive ones.

The potential barrier was also treated as a parameter. Because this barrier is obviously small, the classical approximation for the probability distribution of rotational angle

$$P(\phi) = [\exp(-V(\phi)/RT)]/Q \qquad (3)$$

where $2V(\phi) = V_0(1 - \cos 2\phi)$, is appropriate. We approximated the torsion-sensitive distance distribution by calculating $r_{23}(\phi)$ and $r_{13}(\phi)$ at angle increments $\Delta\phi = 10°$ throughout the range $0° \leq \phi \leq 90°$, weighting each according to $P(\phi)$, and associating with each a "frame" vibrational amplitude. These frame amplitudes were refined as a group, i.e., the differences between them were kept constant. The trial values for them were obtained by interpolation of values calculated[19] for rotamers corresponding to $\phi = 0$, 45, and 90° from a valence-force field taken from the literature.[20]

Results and Discussion

The final results are given in Table I. The interatomic distances of the same type are reasonably consistent, although those from the room-temperature experiment appear to be slightly larger than those from the other two experiments. We do not regard the differences as significant. The theoretical intensity curves and radial distribution curves for the three models defined by Table I are shown in Figures 1–4. Table II is the correlation matrix for the room-temperature results. The other correlation matrices are similar and are available as supplementary material.

The boron–fluorine distance in B_2F_4 is 0.05–0.06 Å shorter than the sum of the covalent single-bond radii corrected for electronegativity difference[21] and the boron–boron distance is some 0.11 Å longer. Considerable double-bond character is thus implied for the B–F link suggesting contributions from structure types I and II which, as far as the BF_2 groups are

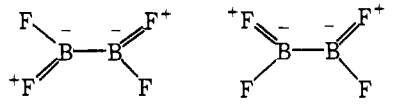

I II

concerned, are the same as those invoked[22] to account for the short bonds (1.3156 ± 0.0044 Å[23]) in BF_3. These structures also account qualitatively for the long B–B bond through the repulsions arising from the unfavorable charge distribution on the boron atoms (surely much reduced by charge transfer to the electronegative fluorine atoms), and the equilibrium coplanarity of the molecule arising from electron delocalization in the conjugated π system of bonds. We note in passing the striking similarities between the structures of B_2F_4 and the isoelectronic molecule N_2O_4[24] which has short N=O bonds, a remarkably long N–N bond, and is planar.

The planar structure of B_2F_4 in the gas contrasts with the staggered conformation of B_2Cl_4. We regard this difference to be the result of a delicate balancing of conjugation favoring the planar form and steric effects favoring the staggered. Conjugation should clearly be more important in B_2F_4 as suggested by its short B–F links than in B_2Cl_4 where the B–Cl bond at 1.750 (0.011) Å is 0.03 Å *longer* than the sum of the covalent single-bond radii corrected for electronegativity difference. On the other hand, steric repulsion between pairs of cis B–F bonds in B_2F_4, although it may be presumed to exist, should be less than that between B–Cl bonds in a hypothetically *planar* form of gaseous B_2Cl_4 derived from the measured staggered form by changing only the torsion angle. (The van der Waals radii offer a part of the basis for this judgment: the cis F ··· F and hypothetical Cl ··· Cl distance in the planar forms are respectively greater than and less than the radius sums.) The length of the B–B bond in staggered B_2Cl_4 is

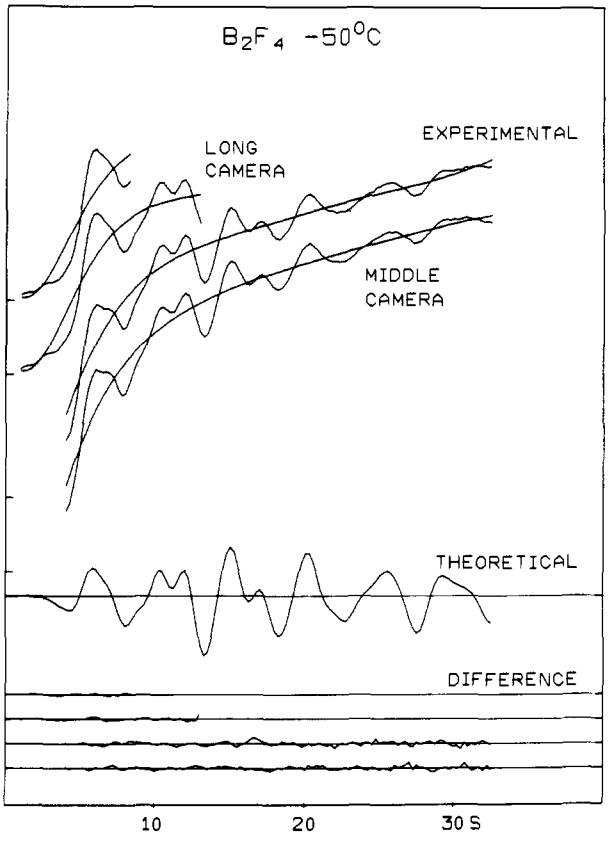

Figure 1. Intensity curves from experiments at −50 °C. The experimental curves are s^4I_{total} shown superposed on the final backgrounds. The theoretical intensity curve is sI_m for the model of Table I. The difference curves are the experimental minus theoretical.

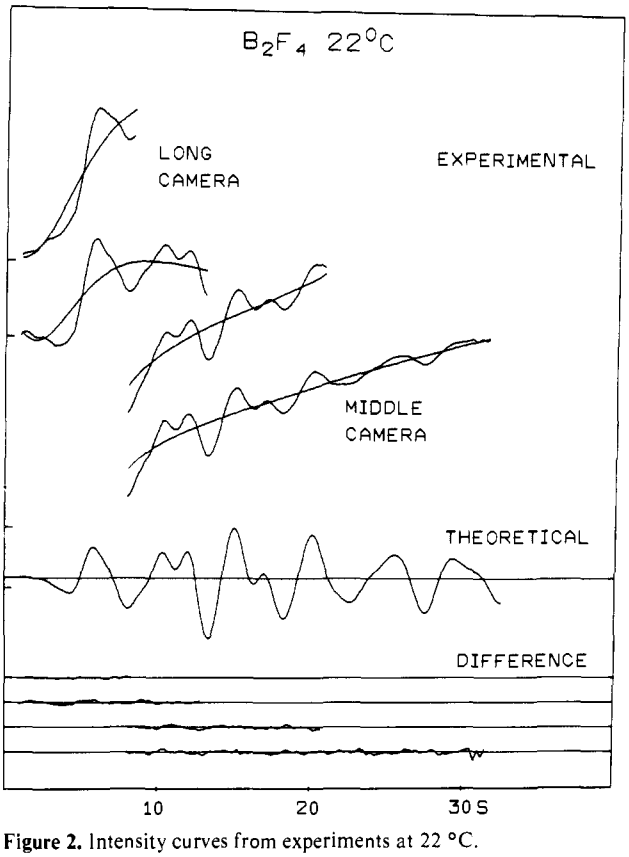

Figure 2. Intensity curves from experiments at 22 °C.

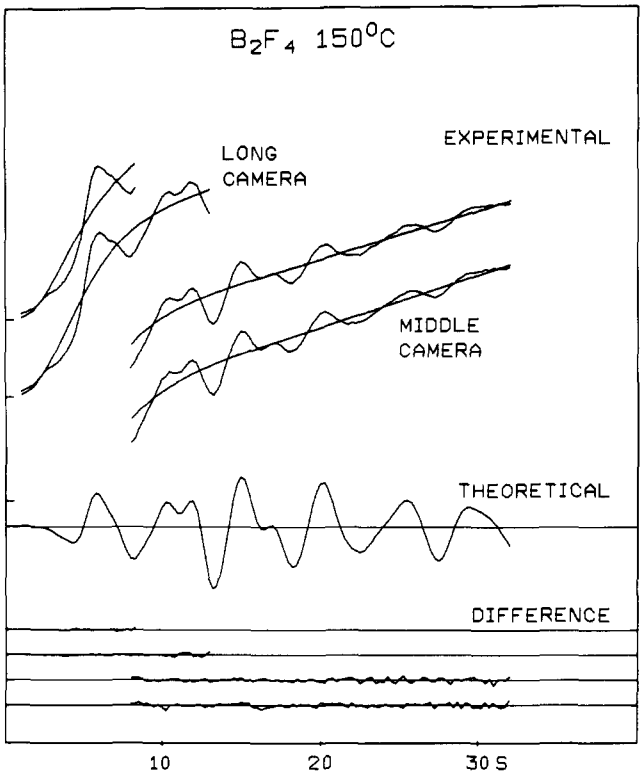

Figure 3. Intensity curves from experiments at 150 °C.

shorter (by 0.018 Å) than in B_2F_4, contrary to expectation based on consideration of conjugation alone. The difference is also consistent with the picture of competitive balancing outlined above. One supposes that both conjugation and bond–bond repusion are operative in B_2F_4 (the latter perhaps because double bonds are more space filling than single bonds), and that both effects are smaller in B_2Cl_4. The longer B–B bond in B_2F_4 reflects a compromise between the small amount of shortening to be expected from conjugation alone and the elongation derived from steric forces.

The structures of a number of molecules with B–B bonds have been measured recently, mostly in the crystal. Of these most have ethane-like configurations in which the geometry of the bonds to boron is roughly tetrahedral.[25] The B–B bond length in such tetrahedrally bonded compounds is on the average substantially longer (ca. 0.08–0.10 Å) than in the trigonally bonded ones[26] and is reminiscent of a qualitatively similar circumstance in carbon compounds. Detailed comparisons of the lengths of trigonal B–B bonds in the crystal with ours for B_2F_4 in the gas phase show them to be in good agreement when account is taken of thermal corrections to the former. Thus, for example, the central bond in phosphorus trifluoride tris(difluoroboryl)borane[26] is 1.6 ± 0.01 Å without thermal corrections estimated to be in the range 0.001–0.013 Å. The agreement between the bond lengths in crystalline B_2F_4 (B–B = $1.67 \pm 0.04_5$ Å, B–F = $1.32 \pm 0.03_5$ Å)[1] and ours for the gas is well within the specified error limits and quite likely would be improved by thermal corrections to the crystal data.

The remarkable temperature dependence of the rotation-sensitive distances, evident in the differing shapes of the radial distribution curves in the region 3.1–3.8 Å, is compatible only with a low rotational barrier. The weighted average of the three values in Table I is 0.42 (2σ = 0.16) kcal/mol, which we take as the best value. If one assumes that the twofold cosine form of the hindering potential can be approximated by the quadratic form $V = V_0\,\phi^2$, one may estimate the fundamental torsional frequency from the relation $\omega = (2\pi c)^{-1}(k_\phi/\mu_l)^{1/2}$ where $k_\phi = 2V_0$ and μ_l is the reduced moment of inertia of the

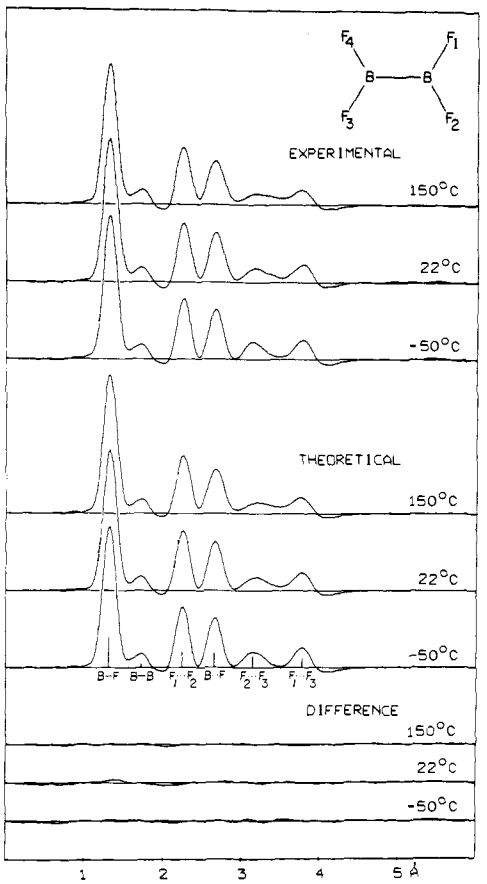

Figure 4. Radial distribution curves. The experimental curves are calculated from composites of the molecular intensities shown in Figures 1-3. The theoretical curves correspond to the models of Table I. The difference curves are experimental minus theoretical.

BF_2 groups. The result is $\omega = 20$ ($2\sigma = 4$) cm^{-1}. From this value and the low barrier one predicts at least seven bound states and high excited state populations even above the barrier. It is not surprising that there is no experimental information about the torsional mode from spectroscopy.

Acknowledgment. This work was supported by the National Science Foundation under Grants No. GP-8453 and CHE 74-13527.

Supplementary Material Available: Tables III and IV (the correlation matrices for the results at −50 and 150 °C) as well as the intensity data and final backgrounds (13 pages). Ordering information is available on any current masthead page.

References and Notes

(1) L. Trefanos and W. N. Lipscomb, *J. Chem. Phys.*, **28**, 54 (1958).
(2) M. Atoji, P. J. Wheatley, and W. N. Lipscomb, *J. Chem. Phys.*, **27**, 196 (1957).
(3) R. R. Ryan and K. Hedberg, *J. Chem. Phys.*, **50**, 4986 (1969).
(4) L. H. Jones and R. R. Ryan, *J. Chem. Phys.*, **57**, 1012 (1972).
(5) J. N. Gayles and J. Self, *J. Chem. Phys.*, **40**, 3530 (1964).
(6) A. Finch, I. Hyams, and D. Steele, *Spectrochim. Acta*, **21**, 1423 (1965).
(7) J. R. Durig, J. W. Thompson, J. D. Witt, and J. D. Odom, *J. Chem. Phys.*, **58**, 5339 (1973).
(8) L. A. Nimon, K. S. Seshadri, R. C. Taylor, and D. White, *J. Chem. Phys.*, **53**, 2416 (1970).
(9) E. B. Moore, Jr., *Theor, Chim. Acta*, **7**, 144 (1967).
(10) A. H. Cowley, W. D. White, and M. C. Damasco, *J. Am. Chem. Soc.*, **91**, 1922 (1969).
(11) M. F. Guest and I. H. Hillier, *Trans. Faraday Soc. II*, **70**, 389 (1974).
(12) J. V. Patton and K. Hedberg, *Bull. Am. Phys. Soc.*, **13**, 831 (1968). The phraseology of this abstract of the report given at the Second Austin Symposium on Gas Phase Molecular Structure unfortunately implies that B_2F_4 has molecular symmetry D_{2d}. The correct symmetry, D_{2h}, was reported at the meeting.
(13) Experimental difficulties at the lowest intended temperature led to long camera plates being made at −80 °C and middle camera plates at −50 °C. The −80 °C data were treated as if they were derived from the higher temperature. These data reflected only low-angle scattering and tests showed that the uncertainties in the parameter values derived from them alone were large enough to justify this simplification.
(14) Beryllium borohydride [G. Gundersen, L. Hedberg, and K. Hedberg, *J. Chem. Phys.*, **59**, 3777 (1973)] and diboron tetrabromide [D. D. Danielson and K. Hedberg, to be published].
(15) G. Gundersen and K. Hedberg, *J. Chem. Phys.*, **51**, 2500 (1969).
(16) L. Hedberg, Abstracts, Fifth Austin Symposium on Gas Phase Molecular Structure, Austin, Tex., Mar 1974, No. T9.
(17) L. Schäfer, A. C. Yates, and R. A. Bonham, *J. Chem. Phys.*, **55**, 3055 (1971).
(18) K. Hedberg and M. Iwasaki, *Acta. Crystallogr.*, **17**, 529 (1964).
(19) For the program used see R. Stølevik, H. M. Seip, and S. J. Cyvin, *Chem. Phys. Lett.*, **15**, 263 (1972). Typical values calculated for l_{13} and l_{23} at 0, 45, and 90° were 0.0871 and 0.1622, 0.0955 and 0.1484, and 0.1195 and 0.1195 at 22 °C.
(20) L. A. Nimon, K. S. Seshadri, R. C. Taylor, and D. White, *J. Chem. Phys.*, **53**, 2416 (1970).
(21) V. Schomaker and D. P. Stevenson, *J. Am. Chem. Soc.*, **63**, 37 (1941). The factor 0.08 instead of 0.09 has been used in the electronegativity correction [L. Pauling, "The Nature of the Chemical Bond", 3rd ed, Cornell University Press, Ithaca, N.Y., 1960, p 229].
(22) L. Pauling, "The Nature of the Chemical Bond", 3rd ed, Cornell University Press, Ithaca, N.Y., 1960, p 317.
(23) S. Konaka, Y. Murata, K. Kuchitsu, and Y. Morino, *Bull. Chem. Soc., Jpn.*, **39**, 1134 (1966).
(24) B. McClelland, G. Gundersen, and K. Hedberg, *J. Chem. Phys.*, **56**, 4541 (1972).
(25) Some examples are bis(carbonyl)diborane(4) [J. Rathke and R. Schaeffer, *Inorg. Chem.*, **13**, 760 (1974)], bis(triphenylphosphine)diborane(4) [W. VanDoorne, A. W. Cordes, and G. W. Hunt, *ibid.*, **12**, 1686 (1973)], and bis(trifluorophosphine)diborane(4) [E. R. Lory, R. F. Porter, and S. H. Bauer, *ibid.*, **10**, 1072 (1971)].
(26) B. G. DeBoer, A. Zalkin, and D. H. Templeton, *Inorg. Chem.*, **8**, 836 (1969).